

## The Intramolecular Sulfur–Nitrogen Bond in Aqueous 3-(Methylthio)propylamine Radical Cation

G. N. R. Tripathi\* and T. Tobien

Radiation Laboratory, University of Notre Dame, Notre Dame, Indiana 46556

Received: October 27, 2000; In Final Form: January 9, 2001

Kinetic and structural properties of the intramolecular sulfur–nitrogen bond ( $>S\cdot:NH_2^{+\cdot-}$ ) in aqueous 3-(methylthio)propylamine (3-MTPA) radical cation have been examined as a model for the cyclized radical state of L-methionine, an essential amino acid in protein biosynthesis. The  $\cdot OH$  radical reacts with amine-protonated 3-MTPA at a rate constant of  $8.3 \times 10^9 M^{-1} s^{-1}$ , primarily by addition at the sulfur site. Intramolecular hydrogen abstraction and water elimination from the  $\cdot OH$  adduct ( $3-MTPAH^+-OH\cdot \rightarrow 3-MTPA^{+\cdot} + H_2O$ ) occurs at a rate of  $9.4 \times 10^7 s^{-1}$ , forming the radical cation. The Raman scattering of 3-MTPA $^{+\cdot}$ , excited in resonance with its broad 390-nm absorption on the microsecond times, exhibits a surprisingly simple spectrum dominated by a strongly enhanced S:N stretching vibration at  $288 cm^{-1}$ , observed for the first time. This observation provides vibrational spectroscopic evidence of intramolecular bonding in 3-MTPA $^{+\cdot}$  and shows that the 390-nm absorption of the radical is almost completely confined to the S:N bond. The equilibrium S–N separation in the radical is estimated as  $\sim 2.5 \text{ \AA}$ . The hypothetical intermediate, SNOH $\cdot$ , presumed to be formed on oxidation of methionine and derivatives in basic solutions, has been identified with the  $>S\cdot:NH^+$ –species.

### Introduction

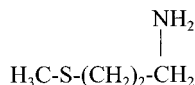
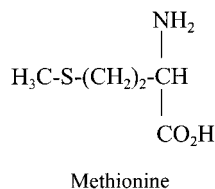
Chemical evidence of a three-electron intramolecular sulfur–nitrogen (S:N) bond in the radical state was first presented by Musker and co-workers in the oxidative cyclization of 5-methyl-1-thia-5-azacyclooctane.<sup>1</sup> A long-lived intermediate produced on reaction of the neutral molecule with its fully oxidized dication form in acetonitrile that gave yellow solution and exhibited broad ESR signals was identified as the S:N bonded radical cation. In a simple description of the nature of the bonding, the S and N radical sites exchange unpaired p and p<sup>2</sup> electrons to form a two-center, three-electron ( $2c/3e$ )  $\sigma^2\sigma^*$  bond.<sup>1–3</sup> Intramolecular interactions of similar nature occur in the oxidized radical states of sulfur-containing amino acids, peptides, and proteins. The sulfur radicals, because of their various biological functions, have been studied extensively for many years, most recently from a kinetic perspective by pulse radiolysis and laser photolysis.<sup>4–8</sup> The S:N bonding is seen as a precursor of decarboxylation in  $\alpha$ -amino acids, an irreversible chemical transformation that changes the protein redox chemistry and enzymatic activity. A wide variation is observed in the chemical reactivity of the S:N bond in different cyclic frames. For example, it is fairly stable in the radical cation of 5-methyl-1-thia-5-azacyclooctane<sup>1</sup> but short-lived in 3-(methylthio)propylamine radical cation.<sup>5–7</sup> Despite the key role of the intramolecularly bonded  $2c/3e$  species in chemically and biologically important reactions, our knowledge of their structural properties is meager. No molecular spectroscopic study of an S:N bonded aqueous species has been reported, to date. The spin-orbit coupling broadens the ESR spectra of sulfur-containing radicals, masking the structural contents.<sup>1,9</sup> Therefore, the structure-reactivity relationship in very few solvated sulfur-radicals has been examined.<sup>10</sup>

Several calculations on  $2c/3e$  polyatomic intermediates have appeared in literature in recent years.<sup>3,11</sup> Comparatively, there

have been few experimental investigations that would allow to test their validity. To our knowledge, the only measurements on bond properties involving  $2c/3e$  sulfur radicals consist of thermal dissociation energies of the intermolecular S:S bonded radical cations in the gas phase and resonance Raman spectra in aqueous solution.<sup>12,13</sup> Correlation has been made between the electronic absorption maxima ( $\lambda_{max}$ ) and thermodynamic stability of some aqueous S:S species.<sup>14</sup> However, the absorption spectra in solution provide little structural insight. Also, they are of little use in predicting the relative stabilities of the solvent-stabilized heteronuclear bonds or geometrically constrained intramolecular bonds.

In radiolytic and photolytic oxidation of aqueous methionine and related amino acids, the appearance of a broad absorption spectrum centered at  $\sim 390$  nm is taken as evidence for the intramolecular  $>S\cdot:NH_2^{+\cdot-}$  bonding.<sup>5–7</sup> This identification is based mainly on a similar absorption seen on one-electron oxidation of 3-(methylthio)propylamine (3-MTPA), of which methionine is a carboxylic acid derivative (Figure 1). 3-MTPA is commonly used as a model compound for unraveling the redox chemistry in sulfur-containing amino acids and peptides.

We have examined, in this work, the formation and structural properties of the 390-nm species, produced by  $\cdot OH$  oxidation of 3-MTPA in aqueous solutions, using transient absorption and time-resolved resonance Raman spectroscopy. The resonance Raman spectra that we observe are extremely simple for a large molecule, such as 3-MTPA $^{+\cdot}$  with no symmetry, and mainly characterize the S:N bond. The stretching and overtone frequencies of the bond have been measured, for which no prior data exist in the literature for comparison. The various theoretical models for the S:N bond structure<sup>11</sup> have been analyzed in view of the spectroscopic information, obtained in this work, to allow a realistic evaluation of the bond length. Kinetic evidence on the disappearance of the 390-nm species in basic solutions has led to the identification of the product species as



3-(Methylthio)propylamine (3-MTPA)

**Figure 1.** 3-(Methylthio)propylamine (3-MTPA) and L-methionine

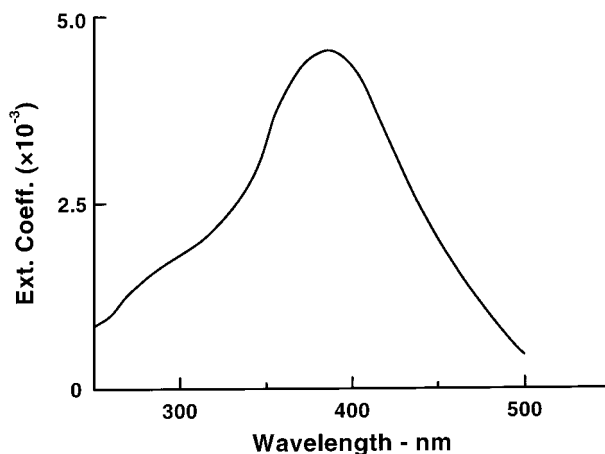
$>\text{S}:\text{NH}^{\bullet-}$ , assigned previously to a hypothetical radical SNOH $^{\bullet}$ .<sup>5</sup> The latter species does not display a recognizable absorption, which has presented difficulties in elucidating the redox chemistry of some biologically important s-amino acids in basic aqueous solutions.

### Experimental Methods

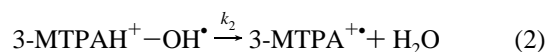
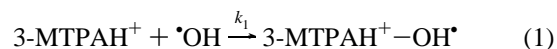
The  $\bullet\text{OH}$  radical produced by pulse radiolysis of water was used to oxidize 3-MTPA ( $\text{p}K_{\text{a}}$  of amine proton 10.5) into its cation radical. On the 100-ns time scale, the radiation yields of  $\bullet\text{OH}$  and hydrated electron ( $e_{\text{aq}}^-$ ) are almost comparable in near neutral oxygen-free water.<sup>15</sup> The  $e_{\text{aq}}^-$  was converted into  $\bullet\text{OH}$  radical by saturating the solution with  $\text{N}_2\text{O}$ . In acidic solutions, the  $\bullet\text{OH}$  yield goes down as  $e_{\text{aq}}^-$  reacts with  $\text{H}^+$  to form hydrated  $\text{H}^{\bullet}$ . The optical absorption and resonance Raman methods applied here to study transient chemical species produced by pulse radiolysis in solution have been described in detail in several previous publications from this laboratory.<sup>16–18</sup> Radiolysis by 8 MeV, 2 ns electron pulses from a new linear accelerator facility in the laboratory, which typically produces a radical concentration of  $\sim 3 \times 10^{-6}$  M per pulse, was used for optical absorption measurements. In Raman experiments, 2 MeV,  $\sim 100$  ns electron pulses, delivered by a Van de Graaff accelerator, at a dose sufficient to produce  $\sim 3 \times 10^{-4}$  M radical concentration per pulse, were applied. The Raman scattering was probed by an excimer laser ( $\sim 100$  mJ) pumped dye laser ( $\sim 10$  ns), tuned in resonance with the optical absorption of the radicals. The spectra were recorded by using an optical multichannel analyzer (OMA) accompanied with an intensified gated diode array detector, with the gate pulse ( $\sim 20$  ns) synchronized with the Raman signal pulse. Extensive signal averaging was performed to improve the signal-to-noise ratio in the Raman spectra, with the accelerator and laser operated at a repetition rate of 7.5 Hz. In both experiments, a flow system was used to refresh the solution between consecutive electron pulses. Raman band positions were measured with reference to the known Raman bands of common solvents, such as ethanol and carbon tetrachloride, and are accurate to within  $\pm 2$   $\text{cm}^{-1}$  for sharp bands and  $\pm 5$   $\text{cm}^{-1}$  for broad and shoulder bands.

### Results and Discussion

**1. Formation Kinetics of 3-MTPA $^{\bullet+}$ .** The  $\bullet\text{OH}$  radical generally reacts with aliphatic molecules by addition or hydrogen (H) atom abstraction.<sup>4</sup> Addition requires the ability to form a covalent bond. In 3-MTPA, the sulfur and amine-N, both have a nonbonding electron pair. Therefore, the  $\bullet\text{OH}$  addition may occur at either site, forming a three-electron bond. Addition at

**Figure 2.** Transient absorption observed 5  $\mu\text{s}$  after electron pulse irradiation of a  $\text{N}_2\text{O}$ -saturated aqueous solution containing 1 mM 3-MTPA at pH 4.3.

the N site is likely to result in H abstraction and  $\text{H}_2\text{O}$  elimination. On amine protonation (3-MTPAH $^+$ ), the  $\bullet\text{OH}$  addition is possible only on the S site (reaction 1). The adduct radicals can undergo  $\text{H}^+/\text{H}_2\text{O}$ -catalyzed loss of water to produce a radical cation (adduct-mediated electron transfer path; AMET).<sup>19</sup> In 3-MTPAH $^+ - \bullet\text{OH}^{\bullet}$ , a  $-\text{NH}_3^+$  proton is readily available to transfer to  $-\text{O}$ , resulting in fast elimination of water and concomitant formation of radical cation (reaction 2).



While the above reaction mechanism is commonly used in the  $\bullet\text{OH}$  oxidation, a precise determination of the rate constants ( $k_1$ ,  $k_2$ ) has not been made previously.<sup>7</sup> These rate constants are essential for understanding the pH dependence of the chemistry. Also, in the absence of kinetic evidence for step 2, oxidation may seem to occur directly via H abstraction. To distinguish between the direct and  $\text{OH}^{\bullet}$  adduct mediated H-abstraction reaction, it is important that the formation kinetics of 3-MTPA $^{\bullet+}$  be monitored at appropriately low ( $k_1[3\text{-MTPA}] \ll k_2$ ) and high ( $k_1[3\text{-MTPA}] \gg k_2$ ) concentrations of 3-MTPA in solution.

Because of experimental convenience, we have used optical absorption for determining  $k_1$  and  $k_2$ . The transient absorption spectrum obtained 5  $\mu\text{s}$  after electron pulse irradiation of a  $\text{N}_2\text{O}$ -saturated aqueous solution containing 1 mM 3-MTPA at pH 4.3 is given in Figure 2. The spectrum is very broad ( $\epsilon_{\text{max}} \sim 4.5 \times 10^3$   $\text{L M}^{-1} \text{cm}^{-1}$  at  $\lambda_{\text{max}} \sim 390$  nm). Temporal evolution of the absorption was monitored at several concentrations of 3-MTPA in solution, from 0.05 mM to 100 mM. At low substrate concentrations, the formation rate increases linearly with concentration (Figure 3a), from which the rate constant,  $k_1$ , was determined as  $8.3(\pm 0.8) \times 10^9$   $\text{M}^{-1}\text{s}^{-1}$ . At high 3-MTPA concentrations, the formation rate (roughly estimated from the first half-period) does not increase linearly (Figure 3b) with concentration, but approaches a plateau, clearly indicating a fast, [3-MTPA]-independent (reaction 2), step in the chemistry. This is the region where the rate of  $\bullet\text{OH}$  reaction with 3-MTPAH $^+$  exceeds the rate of water loss from the OH adduct, and the latter becomes the rate-limiting step. With 100 mM 3-MTPA in solution, the cation radical formation rate ( $\sim 10^8$

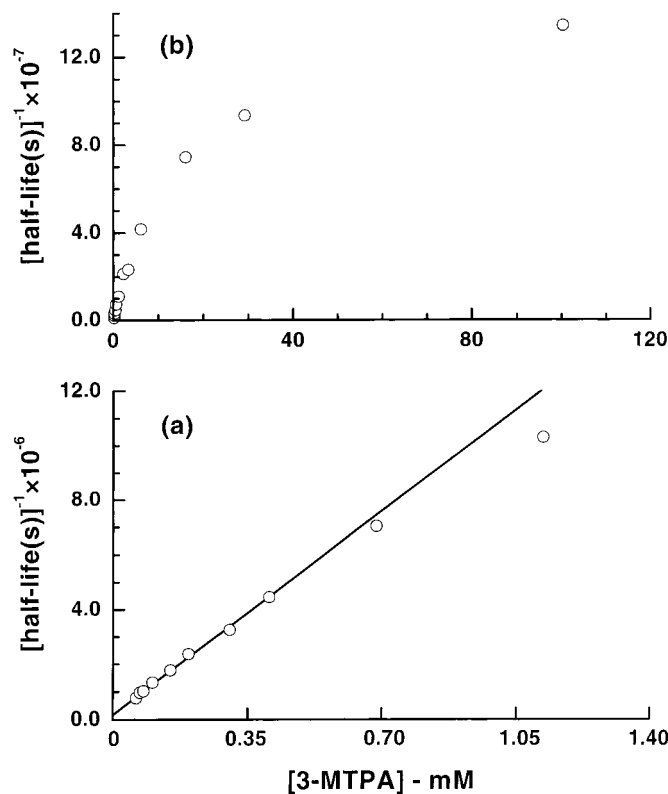


**Figure 3.** The rate (1/first half-period) of formation of the 390-nm transient on electron pulse irradiation of  $\text{N}_2\text{O}$ -saturated aqueous solutions containing 3-MTPA at (a) low and (b) high concentrations at pH 4.3.

$\text{s}^{-1}$ ) is an order of magnitude slower than the rate expected if the reaction 1 was rate limiting. Simulation of the formation kinetics by reactions 1 and 2, with second and first-order rate constants of  $8.3(\pm 0.8) \times 10^9 \text{ M}^{-1} \text{ s}^{-1}$  and  $9.4(\pm 1.3) \times 10^7 \text{ s}^{-1}$ , respectively, gave a good fit with the observed kinetic behavior at all 3-MTPA concentrations.

**2. Nature of the 390-nm Transition.** Knowledge of the nature of the electronic absorption, even if qualitative, is helpful in interpreting the resonance Raman spectra. Calculations performed on 3-MTPA<sup>•+</sup> using various theoretical procedures predict the lowest electronic transition in the 320–372 nm region, the location being sensitive to the S:N bond length.<sup>11</sup> Irrespective of the computational method, the transition is essentially described as one electron promotion from the highest occupied to the lowest unoccupied orbital involving the S and N centers (contribution > 90%). Although calculations on the electronically excited radical have not been performed, the nature of the excited state can be readily inferred from the absorption spectrum. The absorption bandwidth (> 5000  $\text{cm}^{-1}$ ) is too excessive to be contributed entirely by inhomogeneous broadening, and must be attributed, at least in part, to a very short life (<  $10^{-14}$  s) of the excited state. Thus, the excited state is either completely dissociative or very weakly bound. In this respect, the electronic transition in 3-MPTA<sup>•+</sup> resembles that of the diatomic dihalide radical anions.<sup>18,20</sup> A logical role of the “electronically inactive” cyclic molecular frame would be to constrain large amplitude S–N nuclear motions or, in other words, to deepen the potential well.

From the nature of the electronic transition discussed above, one can safely conclude that the equilibrium S–N separation in the excited state geometry must be much larger than in the ground electronic state. Therefore, only those vibrations that involve large S–N displacement are likely to be prominent in

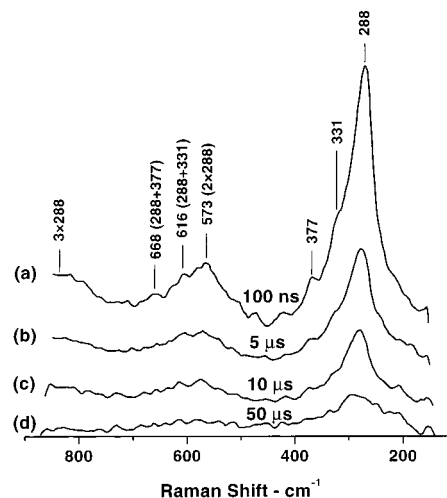


**Figure 4.** Raman spectra obtained by 390-nm excitation on electron pulse irradiation of  $\text{N}_2\text{O}$ -saturated aqueous solution containing 5 mM 3-MTPA at pH 4.3, at different time intervals after the pulse.

resonance Raman. This simple consideration greatly simplifies the interpretation of the resonance Raman spectra. On the other hand, the large spectral width severely dampens the resonance Raman effect,<sup>21</sup> decreasing the spectral enhancement and making the detection of the radical difficult.

**3. Transient Raman Spectra.** The Raman experiments were performed under chemical conditions similar to optical absorption, with 3-MTPA in solution ranging between 2 to 10 mM. The initial observation was made at pH 4.3. The scattering was probed by 390 nm dye laser pulse. The transient Raman signals are weak, as expected, and the principal features occur very close to the excitation wavelength, superimposed over a very strong Rayleigh scattering wing primarily due to water. The spectrometer position was carefully positioned to approach the excitation wavelength within 100  $\text{cm}^{-1}$ , using  $\text{CCl}_4$  Raman signals as reference. The Raman spectra were recorded at several time intervals after electron pulse irradiation of solution, and also without electron pulse. The transient signals that show at microsecond times completely disappear by 500  $\mu\text{s}$ . The time dependence of the transient Raman spectra obtained after digital subtraction of the 500  $\mu\text{s}$  background spectrum is displayed in Figure 4. There was no significant change in the signal intensity for time intervals between 0.1 to 1  $\mu\text{s}$ , suggesting a formation time shorter than  $10^{-7}$  s, consistent with the formation rate determined by kinetic absorption. The experiments were performed in  $\text{H}_2\text{O}$  as well as  $\text{D}_2\text{O}$  solutions to identify the  $-\text{NH}_2$ -sensitive vibrations (Figure 5).

With an initial radical concentration of  $\sim 3 \times 10^{-4}$  M in Raman experiments, a second order decay kinetics is evident from the spectra given in Figure 4. The first half-period of the radical decay, estimated between 4 to 5  $\mu\text{s}$ , gives a second-order rate constant of  $7.5 (\pm 1) \times 10^8 \text{ M}^{-1} \text{ s}^{-1}$ . At this point, we have not confirmed the nature of the product formed by radical–radical reaction. We believe the reaction involves disproportionation, based on an analogy with the intramolecular S:N bonded radical cation observed by Musker and co-workers.<sup>1</sup>

The Raman spectra in Figure 4 display a very prominent band at 288  $\text{cm}^{-1}$ . A weak shoulder band is seen at 331  $\text{cm}^{-1}$ , and an extremely weak band is seen at 377  $\text{cm}^{-1}$ . Overtones of the 288  $\text{cm}^{-1}$  vibration are also observed. Combination bands of the 288  $\text{cm}^{-1}$  vibration with the 331 and 377  $\text{cm}^{-1}$  vibrations also appear in the spectrum, establishing the same molecular species as the origin of the bands. An elementary consideration

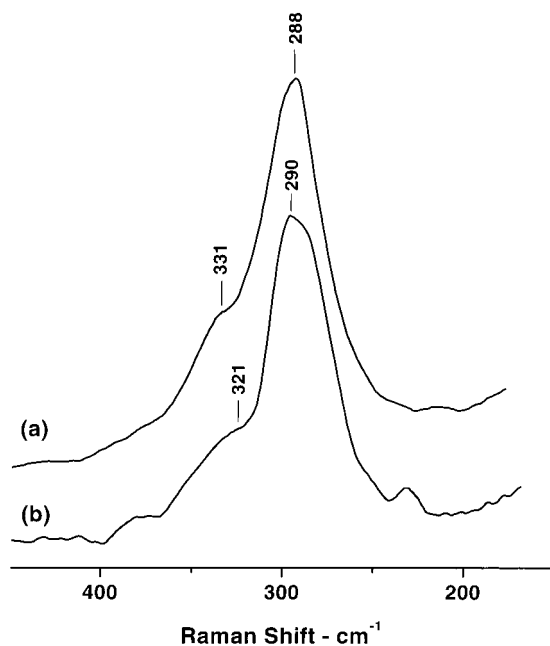


**Figure 5.**  $1\ \mu\text{s}$  390-nm Raman spectrum of 3-MTPA cation radical in: (a)  $\text{H}_2\text{O}$ , (b)  $\text{D}_2\text{O}$ .

of the directed p-valence of the S atom<sup>2</sup> suggests that the S–CH<sub>3</sub> bond may acquire two orientations perpendicular to the S–N bond in 3-MTPA<sup>•+</sup>. The UHF/3-21G\* calculation predicts the energy difference between the two conformers to be small (0.5 kcal mol<sup>-1</sup>), but interconversion is blocked by a barrier of about 5.5 kcal mol<sup>-1</sup>.<sup>11</sup> We do not find any evidence of two conformers in the spectra.

In view of the nature of the resonant electronic transition, the relatively most strongly enhanced 288 cm<sup>-1</sup> band in the spectrum (Figure 4) clearly represents the vibrational mode dominated by the S $\cdots$ N stretch. This frequency is consistent with three-electron bonding between the S and N atoms.<sup>11,18</sup> The 288 cm<sup>-1</sup> frequency is little affected by –NH<sub>2</sub> deuteration (Figure 5). However, the weak shoulder band at 331 cm<sup>-1</sup> drops down in frequency by 10 cm<sup>-1</sup> in D<sub>2</sub>O. The vibrations involving ring distortion, particularly the bond angles connecting S and N atoms to adjacent C atoms, should contain a small S $\cdots$ N stretching component to keep the center of mass stationary during the oscillations. This approximate description applies to the 331 and 371 cm<sup>-1</sup> modes, as they would also involve motion of the NH<sub>2</sub> protons that would make them sensitive to deuteration.<sup>22</sup> It is clear from the intensity pattern of the spectrum that there is very little mechanical coupling between the S $\cdots$ N stretch and other nuclear motions.

Anharmonicity in the 288 cm<sup>-1</sup> mode, if any, is small. Due to broad overtone bands, an accurate determination of this spectroscopic parameters was not possible. The first-order anharmonicity is probably close to 1.5 cm<sup>-1</sup>, which for a diatomic species would amount to a dissociation energy of  $\sim 1.7$  eV, considering a Morse potential energy surface. However, such estimation is of little quantitative significance in a polyatomic molecule. It does indicate, however, that the potential energy well for the S $\cdots$ N stretching mode is not too shallow for bond dissociation to occur at room temperatures.

The spectra in Figure 4 are surprisingly simple for a radical with 45 Raman-active vibrations. The lack of significant mechanical coupling makes the S $\cdots$ N frequency ideally suited for comparing the bond strengths in radicals derived from different sulfur amino acids, peptides, and proteins, where such a linkage occurs.

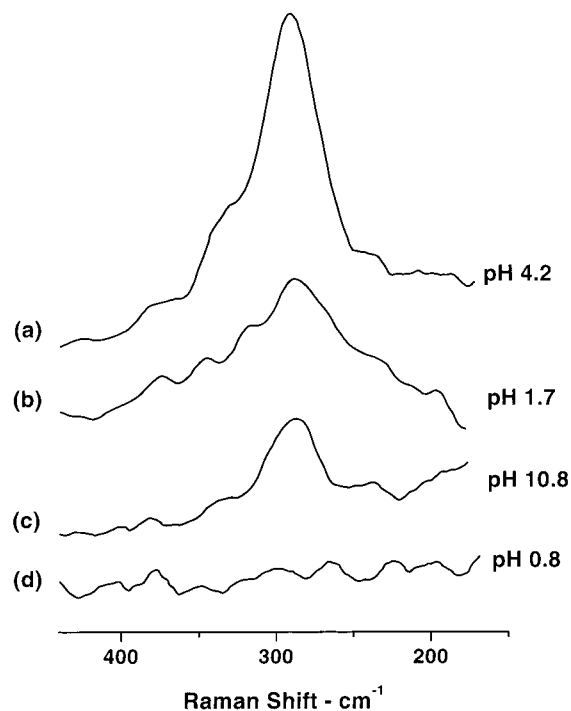


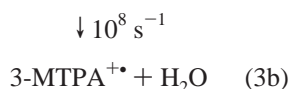
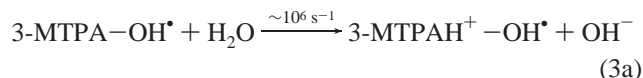
**Figure 6.** pH dependence of the  $0.5\ \mu\text{s}$  390-nm Raman spectrum of the 3-MTPA cation radical obtained on electron pulse irradiation of N<sub>2</sub>O-saturated aqueous solutions containing 5 mM 3-MPTA.

**4. The pH Dependence of 3-MTPA<sup>•+</sup> Formation.** *Acidic Solutions.* The  $0.5\ \mu\text{s}$  Raman spectra of the 390-nm transient were probed at several pH, from 1 to 12. There is very little variation in the signal intensity between pH 4.2 to 9. At lower pH, the radiation yield of  $\bullet\text{OH}$  goes down, as the  $e_{\text{aq}}^-$  starts reacting with  $\text{H}^+$  (rate constant  $2.3 \times 10^{10}\ \text{M}^{-1}\ \text{s}^{-1}$ ).<sup>15</sup> Thus,  $e_{\text{aq}}^-$  does not convert completely into  $\bullet\text{OH}$  by reaction with N<sub>2</sub>O-saturated (26 mM) water (rate of  $2.6 \times 10^8\ \text{s}^{-1}$ ). At pH 1.7, only 36% of  $e_{\text{aq}}^-$  converts to  $\bullet\text{OH}$ , and the rest reacts with  $\text{H}^+$ . Therefore, the  $\bullet\text{OH}$  yield at pH 1.7 is estimated to be about 68% of the yield at pH 4.3. The observed Raman signals, scaled up to compensate for the lower yield, are shown in Figure 6b. It can be seen that the signal intensity at pH 1.7 is still only 40(±5)% of the intensity at pH 4.3. At pH 0.8, no transient Raman signal is observed. Obviously, there is competition between the reaction of 3-MTPAH<sup>+</sup>–OH $\bullet$  with the proton ( $\text{H}_3\text{O}^+$ ) in water and intramolecular  $\text{H}^+$  abstraction (reaction 2; rate  $9.4 \times 10^7\ \text{s}^{-1}$ ) that forms cyclic 3-MTPA<sup>•+</sup>. The 40% yield of 3-MTPA<sup>•+</sup> at pH 1.7 gives a rate constant of  $7(\pm 1) \times 10^9\ \text{M}^{-1}\ \text{s}^{-1}$  for the reaction of 3-MTPAH<sup>+</sup>–OH $\bullet$  with  $\text{H}_3\text{O}^+$ .

*Basic Solutions.* Progressively faster decay of the 390 nm species with pH in basic solutions is fairly common in photooxidized s-amino acids.<sup>5,6</sup> Several mechanism have been proposed to account for the observation.<sup>5,6</sup> The question relates to the nature of the transient formed on decay, as the absorption spectrum of the product species is not seen. The resonance Raman spectrum of 3-MTPA<sup>•+</sup>, produced by  $\bullet\text{OH}$  oxidation, was scanned at pH > 10 to confirm the trend. Figure 6c depicts the  $0.5\ \mu\text{s}$  spectrum at pH 10.8, which is only  $\sim 30\%$  as strong as that at pH 4.2. The Raman signals become unobservable at pH 11.5.

If  $\bullet\text{OH}$  addition occurred at the S site of the neutral 3-MTPA, it is likely that the OH<sup>-</sup> elimination would be a slow ( $\gg 1\ \mu\text{s}$ ) process, as the proton is not readily available to catalyze the reaction.<sup>4</sup> However, that does not explain the loss of 3-MTPA<sup>•+</sup> signals at pH 10.8. 3-MTPA–OH $\bullet$  would rapidly react with water

(rate  $>10^6 \text{ s}^{-1}$ )<sup>23</sup> to form 3-MTPAH<sup>+</sup>–OH<sup>•</sup> (reaction 3), assuming  $pK_a$  of the amine proton in the OH adduct to be similar to that of the parent molecule. Because 3-MTPAH<sup>+</sup>–OH<sup>•</sup> converts into radical cation at a rate of  $\sim 10^8 \text{ s}^{-1}$ , a decrease in the cation radical yield at 0.5  $\mu\text{s}$  is not expected at pH 10.8 (reaction 3). A significant drop in the cation radical yield would be seen at a pH well above the  $pK_a$  of the parent molecule

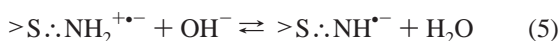


when the rate of reaction of OH<sup>−</sup> with 3-MTPAH<sup>+</sup>–OH<sup>•</sup> (back reaction 3a) becomes comparable to that of the water loss from the species (3a–3b).

An explanation in terms of deprotonation of the radical cation (390 nm species) in basic solutions can be given. However, that implies that  $pK_a$  of 3-MTPA<sup>+</sup>• is similar to that of the parent molecule. Unfortunately, we could not produce 3-MTPA<sup>+</sup>• by direct electron transfer, using N<sub>3</sub><sup>•</sup> or SO<sub>4</sub><sup>•−</sup> as oxidants, which would allow us to determine its  $pK_a$ . Because the observed drop in the 3-MTPA<sup>+</sup>• yield may depend on the mode of the •OH attack on the neutral molecule and properties of the adduct radicals, a definite conclusion cannot be reached using •OH oxidation. Fortunately, the kinetic behavior of the 390-nm intermediate, produced by sensitized photooxidation of some *s*-amino acids in basic solutions, is known. In aqueous methionylglycine,<sup>5</sup> the fast decay rate ( $k_{\text{fast}}$ ) was found to depend on the OH<sup>−</sup> concentration by the following relation:

$$k_{\text{fast}} = 6 \times 10^9 [\text{OH}^-] \text{ s}^{-1} + 1.3 \times 10^6 \text{ s}^{-1} \quad (4)$$

This relationship is typical of the acid–base equilibrium.<sup>24</sup> The base-dependent rate ( $6 \times 10^9 [\text{OH}^-] \text{ s}^{-1}$ ) corresponds to the reaction of the 390-nm transient ( $>\text{S}:\text{NH}_2^{+\bullet}$ ) with OH<sup>−</sup> (forward reaction 5):



The constant rate term ( $1.3 \times 10^6 \text{ s}^{-1}$ ) represents the back reaction involving deprotonated species ( $>\text{S}:\text{NH}^{\bullet-}$ ) and water. These rates lead to a  $pK_a$  of 10.3 for the intermediate. Reaction 5 explains why the equilibrium concentration of  $>\text{S}:\text{NH}_2^{+\bullet}$  decreases with pH, as noted previously. The slow component in the decay kinetics pertains to the second-order decay of the  $>\text{S}:\text{NH}_2^{+\bullet}$  equilibrium concentration. Thus, the hypothetical radical SNOH<sup>•</sup>,<sup>5</sup> assigned previously to the reaction product of  $>\text{S}:\text{NH}_2^{+\bullet}$  and OH<sup>−</sup>, can be identified with the basic form of the 390-nm species with certainty. The  $pK_a$  of the  $>\text{S}:\text{NH}_2^{+\bullet}$  moiety in 3-MTPA<sup>+</sup> is likely to be of comparable magnitude, which explains the 0.5  $\mu\text{s}$  Raman signal intensities at pH 10.8 and 11.5.

The low  $pK_a$  of the  $>\text{S}:\text{NH}_2^{+\bullet}$  species suggests that the positive charge is mostly on the nitrogen atom.<sup>2,25</sup>

**5. The S:N Bond Length in Aqueous 3-MTPA<sup>+</sup>•.** Theoretical structure calculations provide a means of converting the experimental vibrational frequencies of reactive intermediates into bond lengths and bond angles. Unfortunately, none of the calculations<sup>11</sup> on the S:N stretching mode of 3-MTPA<sup>+</sup>•<sup>11</sup> provide a satisfactory description of the observed frequency in water. The UHF/3-21G\* procedure was used to explore the effect of solvation, using a simple Onsager reaction field model.

It was predicted that a small upward shift of 6  $\text{cm}^{-1}$  in frequency might occur due to hydration. On that basis, solvation as a major cause of disagreement between the observed and calculated frequency was ruled out. SCF structural optimizations using larger basis sets or density functional (DFT) procedures, such as UB3LYP/6-311(d,p), predict vibrational frequencies that are far lower than the experimental S:N frequency in 3-MTPA<sup>+</sup>•. However, there is some consistency between the S:N frequencies and bond lengths, calculated by different methods, which can be used. For instance, if a particular computation method predicts a frequency that is  $\Delta\nu$  ( $\text{cm}^{-1}$ ) higher, it also predicts a bond that is shorter ( $\Delta R$ ) by approximately  $0.002 \times \Delta\nu$  ( $\text{\AA}$ ).<sup>26</sup> This empirical relationship allows extrapolating the bond length to correspond to the experimental frequency.

In view of the above empirical relationship, the experimental S:N frequency of 288  $\text{cm}^{-1}$  in 3-MTPA<sup>+</sup>• would correspond to a bond length of  $\sim 2.52 \text{ \AA}$ , if the UB3LYP/6-311(d,p) frequency (256  $\text{cm}^{-1}$ ) and bond length (2.58  $\text{\AA}$ ) are used as reference. Alternatively, one can use UQCISD/6-311(d,p) bond length (2.44  $\text{\AA}$ ) and frequency (331  $\text{cm}^{-1}$ ) as reference to get about the same value. In the absence of reliable calculations, this empirical relationship should be useful in comparing the S:N bond lengths in aqueous radicals, using the observed frequencies.

**6. Bond Properties and Thermochemistry.** An insight into the contrasting thermochemical behavior of the intramolecular S:N bond in 3-MTPA<sup>+</sup>• and intermolecular S:S bond in tetramethyldisulfide radical cation (TMDS<sup>+</sup>•) in aqueous solutions can be gained by a qualitative consideration of the bond properties, based on the vibrational frequencies and anharmonicity constants.

The fact that the S:N stretching motion in 3-MTPA<sup>+</sup>• does not couple significantly with other nuclear motions in the molecule suggests that the observed frequency cannot be significantly different from that of an isolated S:N bond of identical structural properties. With this approximation, we compare the strength of the bond with those in diatomic dihalide anion radicals.<sup>18,20</sup> The vibrational frequencies in Cl<sub>2</sub><sup>•−</sup> (274  $\text{cm}^{-1}$ ), Br<sub>2</sub><sup>•−</sup> (168  $\text{cm}^{-1}$ ), and I<sub>2</sub><sup>•−</sup> (115  $\text{cm}^{-1}$ ),<sup>20</sup> if multiplied by the square root of their reduced masses,<sup>27</sup> predict the bond energies (29.1, 26.2, and 24.3  $\text{kcal mol}^{-1}$ , respectively) reasonably well.<sup>3</sup> Assuming a similar behavior, the bond energy for a vibrational frequency of 288  $\text{cm}^{-1}$  comes out to be  $\sim 1 \text{ eV}$  (23  $\text{kcal mol}^{-1}$ ). This value is about half the bond energy of a single S–N (45  $\text{kcal mol}^{-1}$ ) bond, estimated from the formation energies of S and N atoms, which is generally a characteristic of the three-electron bonds.<sup>2</sup>

An uncoupled S:N frequency of 288  $\text{cm}^{-1}$  would correspond to an S:S frequency of 225  $\text{cm}^{-1}$ , if N is replaced by heavier S, without changing the bond properties. The 276  $\text{cm}^{-1}$  S:S mode in TMDS<sup>+</sup>• is weakly coupled with the symmetric methyl-wagging vibration ( $\delta_s\text{S-CH}_3$ ) that produces another mode containing an S:S stretch at 157  $\text{cm}^{-1}$ .<sup>13,28</sup> Mechanical coupling increases the frequency separation between the uncoupled modes. Because the 276  $\text{cm}^{-1}$  mode is about four times more strongly enhanced, the uncoupled S:S frequency should be closer to or slightly lower than 276  $\text{cm}^{-1}$  ( $\sim 250 \text{ cm}^{-1}$ ). Considering the uncoupled frequency in the range of 250–276  $\text{cm}^{-1}$ , the S:S bond energy in TMDS<sup>+</sup>• (25.6–28.3  $\text{kcal mol}^{-1}$ ) is estimated to be greater than the S:N bond energy in 3-MTPA<sup>+</sup>• by 10 to 19%. This is not surprising, as the bond energy of a single S–S bond (51  $\text{kcal mol}^{-1}$ ) is about  $\sim 12\%$

higher than that of a single S–N bond. Theoretical calculations also predict weaker three-electron bonds between dissimilar atoms.<sup>2,3</sup>

The bond dissociation energy in a polyatomic molecule can be higher or lower than the bond energy, depending on whether the other bonds are weakened or strengthened during the dissociation process.<sup>2</sup> In aqueous dihalide radical ions, the bond dissociation energies estimated from the vibrational anharmonicities are comparable to the gas-phase bond energies, suggesting that bonding with the water molecules has only a small effect.<sup>18,20</sup> For an isolated S:N bond of 288 cm<sup>-1</sup> frequency, one would expect an anharmonicity constant of ~2.6 cm<sup>-1</sup>, assuming a bond energy of ~1 eV. Because the observed anharmonicity (~1.5 cm<sup>-1</sup>) is lower, the bond dissociation energy is very likely greater, and not lower, than the bond energy. Therefore, thermochemical dissociation is not likely to play a significant role in the aqueous chemistry of 3-MTPA<sup>+</sup> at room temperatures, which is consistent with the observations. A similar conclusion can be drawn from the high rate of radical cyclization (>10<sup>8</sup> s<sup>-1</sup>) on oxidation of 3-MTPA.<sup>29</sup> We attribute this property to the structural constraint of the cyclic molecular frame.

Now let us consider bond dissociation in noncyclic aqueous TMDS<sup>+</sup>. The 157 cm<sup>-1</sup> S:S mode of the radical, which contains a large  $\delta_s$ S–CH<sub>3</sub> component, is very anharmonic in water, and how this behavior relates to the solvent interactions is being investigated.<sup>28</sup> At this point, it would suffice to say that an extrapolation based on the observed anharmonicity gives an energy of 0.55 eV (12.6 kcal mol<sup>-1</sup>) for the 157 cm<sup>-1</sup> mode to disappear, which coincides with the thermal dissociation energy of the aqueous TMDS<sup>+</sup>.<sup>30</sup> The experimental gas-phase dissociation energy of TMDS<sup>+</sup> is about twice as large (27.5 kcal mol<sup>-1</sup>).<sup>12</sup> The low value of the S:S dissociation energy in water suggests that the excess bond energy is used in bonding with the water molecules in which the free methyl bending motion plays a role.<sup>28</sup>

The above discussion, although qualitative, leads to the interesting conclusion that it is the chemical environment rather than the bond strength that accounts for the greater thermochemical stability of the S:N bond in 3-MTPA<sup>+</sup>, as compared to the S:S bond in TMDS<sup>+</sup>, in water.

## Summary

The vibrational characteristics of a >S:NH<sub>2</sub><sup>+-</sup> bond have been reported for the first time. A variety of sulfur-containing amino acids exist in nature, with the possibility of forming intramolecular sulfur–nitrogen bonds of different strengths in their redox intermediate state. Direct experimental evidence for the bonding can come from time resolved resonance Raman spectroscopy, as shown in this work. The frequency of the S:N stretching mode in aqueous 3-(methylthio)propylamine radical cation (3-MPTA<sup>+</sup>) will provide a standard for comparing the bond strength in different molecular environments.

It has been recognized, for the first time, that the intramolecular >S:NH<sub>2</sub><sup>+-</sup> species undergoes deprotonation at a surprising low pH, a finding that would be of importance in understanding the redox chemistry of sulfur amino acids in basic solutions. Contrary to the common perception, the thermochemical stability of the S:N bond in 3-MPTA<sup>+</sup> does not arise from the bond strength, but from the structural constraints. The S:S bond in tetramethyldisulfide radical cation (TMDS<sup>+</sup>) is relatively stronger, but it undergoes thermochemical dissociation at room temperatures due to interaction with the water molecules.

**Acknowledgment.** The research described herein was supported by the Office of Basic Energy Sciences of the Department of Energy. This is Contribution No. NDRL-4265 from the Notre Dame Radiation Laboratory. One of the authors (G.N.R.T.) thanks Drs. K. Bobrowski and G. L. Hug for useful discussions on the kinetic behavior of the >S:NH<sub>2</sub><sup>+-</sup> species derived from methionylglycine in basic solutions.

## References and Notes

- (1) Musker, W. K.; Hirschon, A. S.; Doi, J. T. *J. Am. Chem. Soc.* **1978**, *100*, 7754. Musker, W. K.; Surdhar, P. S.; Ahmad, R.; Armstrong, D.A. *Can. J. Chem.* **1984**, *62*, 1874.
- (2) Pauling, L. *The Nature of the Chemical Bond*; Cornell University Press: Ithaca, New York, 1960. Pauling, L. *J. Am. Chem. Soc.* **1931**, *53*, 3225.
- (3) Clark, T. *J. Am. Chem. Soc.* **1988**, *110*, 1772 and references therein.
- (4) Sonntag, C. v. *The Chemical Basis of Radiation Biology*; Taylor and Francis: New York, 1987.
- (5) Hug, G. L.; Marciniak, B.; Bobrowski, K. *J. Phys. Chem.* **1996**, *100*, 14914, and references therein.
- (6) Hug, G. L.; Marciniak, B.; Bobrowski, K. *J. Photochem. Photobiol. A* **1996**, *95*, 81. Marciniak, B.; Hug, G. L.; Bobrowski, K.; Halina, K. *J. Phys. Chem.* **1995**, *99*, 13560. Bobrowski, K.; Marciniak, B.; Hug, G. L.; Halina, K. *J. Phys. Chem.* **1994**, *98*, 537.
- (7) Asmus, K.-D.; Gobl, M.; Hiller, K.-O.; Mahling, S.; Monig, J. *J. Chem. Soc., Perkin Trans. 2* **1985**, 641. Hiller, K.-O.; Masloch, B.; Gobl, M.; Asmus, K. D. *J. Am. Chem. Soc.* **1981**, *103*, 2734 and references therein.
- (8) Armstrong D. A.; Sun, Q.; Tripathi, G. N. R.; Schuler, R. H.; McKinnon, D. *J. Phys. Chem.* **1993**, *97*, 5611.
- (9) Champagne, M. H.; Mullins, M. W.; Colson, A.-O.; Sevila, M. D. *J. Phys. Chem.* **1991**, *95*, 6487.
- (10) Tripathi, G. N. R.; Chipman, D. M.; Schuler R. H. *J. Phys. Chem.* **1995**, *99*, 5264. Tripathi, G. N. R.; Sun, Q.; Armstrong, D. A.; Chipman, D. M.; Schuler, R. H. *J. Phys. Chem.* **1992**, *96*, 5344.
- (11) Carmichael, I. *Acta Chim. Scand.* **1997**, *51*, 567.
- (12) Deng, Y.; Illies, J.; James, M. A.; McKee, M. L.; Peschke, M. *J. Am. Chem. Soc.* **1995**, *117*, 420.
- (13) Wilbrandt, R.; Jensen, N. H.; Pagsberg, P.; Sillesen, A. H.; Hansen, K. B.; Hester, R. E. *J. Raman Spectrosc.* **1981**, *11*, 24. Wilbrandt, R.; Jensen, N. H.; Pagsberg, P.; Sillesen, A. H.; Hansen, K. B.; Hester, R. E. *Chem. Phys. Lett.* **1979**, *80*, 315. Jensen, N. H.; Wilbrandt, R.; Pagsberg, P.; Hester, R. E.; Ernstbrunner, E. *J. Chem. Phys.* **1979**, *71*, 3326.
- (14) Gobl, M.; Bonifacic, M.; Asmus, K.-D. *J. Am. Chem. Soc.* **1984**, *106*, 5884.
- (15) Buxton, G. V.; Greenstock, C. L.; Helman, W. P.; Ross, A. B. *J. Phys. Chem. Ref. Data* **1988**, *17*, 513.
- (16) Patterson, L. K.; Lilie, J. *Int. J. Radiat. Phys. Chem.* **1974**, *6*, 129.
- (17) Tripathi, G. N. R. In *Multichannel Image Detectors II*; Talmi, Y., Ed.; ACS Symposium Series 236; American Chemical Society: Washington, DC, 1983; p 171.
- (18) Tripathi, G. N. R. In *Advances in Spectroscopy Vol. 18, Time-Resolved Spectroscopy*; Clark, R. J. H., Hester, R. E., Eds.; John Wiley & Sons: New York, 1989; pp 157–218.
- (19) Tripathi, G. N. R. *J. Am. Chem. Soc.* **1998**, *120*, 4161.
- (20) Tripathi, G. N. R.; Schuler, R. H.; Fessenden, R. W. *Chem. Phys. Lett.* **1985**, *113*, 563.
- (21) Albrecht, A. C.; Hutley, M. C. In *Raman Spectroscopy*; Szymanski, H. A., Ed.; Plenum: New York, 1970; Vol. 2, p 33. Albrecht, A. C.; Hutley, M. C. *J. Chem. Phys.* **1971**, *55*, 4438.
- (22) Tripathi, G. N. R. *J. Chem. Phys.* **1980**, *73*, 5521.
- (23) The rate of reaction of OH<sup>-</sup> taken as ~10<sup>10</sup> [OH<sup>-</sup>]<sup>-1</sup> s<sup>-1</sup>, which gives the rate of reaction of deprotonated species with water as ~10<sup>10</sup> [10<sup>pK<sub>a</sub>-14</sup>] s<sup>-1</sup>.
- (24) Bell, R. P. *The Proton in Chemistry*; Cornell University Press: Ithaca, New York, 1959.
- (25) Tripathi G. N. R., Su Y. *J. Am. Chem. Soc.* **1996**, *118*, 2235. Tripathi, G. N. R.; Su, Y.; Bentley, J. *J. Am. Chem. Soc.* **1995**, *118*, 2235. Tripathi, G. N. R.; Su Y.; Bentley J.; Fessenden, R. W.; Jiang, P.-Y. *J. Am. Chem. Soc.* **1996**, *118*, 2245. These papers discuss proton reactivity of radicals containing nitrogen atom.
- (26) A linear relationship is a valid approximation only when the change in  $\nu$  is small. In view of Badger's relation (reference 2),  $\Delta(\text{bond length}) \propto -\Delta\nu/\nu^2$  applies to bonds of drastically different strengths.
- (27) For this qualitative discussion, the bond energy (kcal mol<sup>-1</sup>) is related to the vibrational frequency,  $\nu(\text{cm}^{-1})$ , by 0.0256  $\nu\mu^{1/2}$ , where  $\mu$  is reduced mass in atomic units. Using experimental  $\nu$  values in water, which may be slightly different from the gas phase, one estimates the bond energies for Cl<sub>2</sub><sup>•+</sup>, Br<sub>2</sub><sup>•+</sup>, I<sub>2</sub><sup>•+</sup>, and (CH<sub>3</sub>)<sub>2</sub>S<sub>2</sub><sup>•+</sup>(TMDS<sup>+</sup>) as 29.5, 26.8, 23.6, and 28.2 kcal mol<sup>-1</sup>, respectively, which compare well with the experimental values (29.1, 26.2, 24.3, and 27.5 kcal mol<sup>-1</sup>) in the gas phase (ref. 3, 12).

(28) Frequencies given here are from our own work, which we consider to be more precise than the literature values (reference 13). Combination bands of the  $276\text{-cm}^{-1}$  mode with  $157\text{-cm}^{-1}$  appear at frequencies,  $\nu\text{ (cm}^{-1}\text{)} = 276\nu + (157 - 10\nu)$ . The series converges for an extrapolated energy of  $0.55\text{ eV}$  ( $12.6\text{ kcal mol}^{-1}$ ) ( $\nu \sim 16$ ). The molecular mechanism of  $\text{S}:\text{S}$  bond dissociation in aqueous  $\text{TMDS}^{+\bullet}$  is not yet clear. The extrapolated disappearance of the  $157\text{-cm}^{-1}$  mode in  $\text{TMDS}^{+\bullet}$  suggests "free" symmetric

$-\text{S}-\text{CH}_3$  wagging motion which apparently facilitates  $(\text{CH}_3)_2\text{S}^+:\text{OH}_2$  bonding  $[(\text{CH}_3)_2\text{S}:\text{S}(\text{CH}_3)_2]^{+\bullet}-\text{OH}_2 \rightarrow (\text{CH}_3)_2\text{S}:\text{OH}_2^{+\bullet} + (\text{CH}_3)_2\text{S}]$ .

(29) The  $\text{S}:\text{N}$  bond is likely to form instantaneously upon removal of an electron from S or N. Therefore, it can be safely stated that the formation rate is faster than  $k_2$  ( $\sim 10^8\text{ s}^{-1}$ ).

(30) Monig, J.; Goslich, R.; Asmus, K-D. *Ber. Bunsen-Ges. Phys. Chem.* **1986**, *90*, 115.